Sinapic Acid Attenuated Cardiac Remodeling After Myocardial Infarction by Promoting Macrophage M2 Polarization Through PPARγ Pathway

Mei Yang
Renmin Hospital of Wuhan University: Wuhan University Renmin Hospital https://orcid.org/0000-0002-0376-6592

Jun Xiong
Renmin Hospital of Wuhan University: Wuhan University Renmin Hospital

Qiang Zou
Renmin Hospital of Wuhan University: Wuhan University Renmin Hospital

Xi Wang
Renmin Hospital of Wuhan University: Wuhan University Renmin Hospital

Ke Hu
Renmin Hospital of Wuhan University: Wuhan University Renmin Hospital

Qingyan Zhao (ruyan71@163.com)
Renmin Hospital of Wuhan University: Wuhan University Renmin Hospital

Research Article

Keywords: Sinapic acid, myocardial infarction, macrophage, interstitial fibrosis, PPARγ

Posted Date: January 27th, 2022

DOI: https://doi.org/10.21203/rs.3.rs-1240336/v1

Abstract

Background Macrophage polarization is one of the important regulatory mechanisms of ventricular remodeling. Studies have shown sinapic acid (SA) exerts an anti-inflammatory role. However, the effect of SA on macrophage is still unclear. The purpose of the study was to investigate the role of SA in macrophage polarization and ventricular remodeling after myocardial infarction (MI).

Methods and results MI model was established by ligating left coronary artery. The rats with MI were treated with SA for 1 week or 4 weeks after MI. The effect of SA on bone marrow-derived macrophages (BMDMs) was also observed in vitro. Cardiac systolic dysfunction was significantly improved after SA treatment. SA reduced MCP-1 and CCR2 expressions and macrophage infiltration. SA decreased inflammatory factors TNF-α, IL-1α and IL-1β levels and increased M2 macrophage marker CD206, Arg-1 and IL-10 levels at 1 week after MI. Myocardial interstitial fibrosis and MMP-2 and MMP-9 levels were declined, and sympathetic nerve marker TH and nerve sprouting marker GAP43 were suppressed after SA treatment at 4 weeks after MI. PPARγ level was notablely upregulated after SA treatment. In vitro, SA also increased expression of PPARγ mRNA in BMDMs and IL-4 induced BMDMs in a concentration-dependent manner. SA enhanced Arg1 and IL-10 expressions in BMDMs and the PPARγ antagonist GW9662 attenuated M2 macrophage markers expressions.

Conclusions Our results demonstrated that SA attenuated structural and neural remodeling by promoting macrophage M2 polarization via PPARγ activation after MI.

Introduction

Monocytes were recruited to the necrosis and ischemia myocardium and then become plastic macrophages after myocardial infarction (MI). A few days in the early stage of MI polarized M1 macrophages secrete pro-inflammatory mediators to activate an intense inflammatory cascade response, and polarized M2 macrophages persist for weeks to participate in fibrosis and remodeling [1]. Interstitial fibrosis after MI is the main cause of heart failure and sympathetic neural remodeling contributes to ventricular arrhythmia that is closely associated with sudden cardiac death (SCD) [2, 3]. Studies have shown that modulation of macrophage polarization is a potential therapeutic target for cardiac remodeling after MI [4].

Sinapic acid (SA) is a hydroxycinnamic acid derivative that has a variety of biological effects, such as antioxidant, anti-inflammatory and anticancer activities. Studies have shown that SA plays an anti-inflammatory role in renal and hepatic injury [5, 6]. Recently, one study found that SA could ameliorate acute DOX-induced cardiotoxicity by inhibiting inflammation [7]. Furthermore, SA protected hypertension by modulating reactive oxygen species and inhibiting fibrosis [8, 9]. SA also has antilipidemic and antioxidant effects in the early stage of myocardial damage [10, 11]. However, the effects of SA on macrophage polarization and cardiac remodeling after MI have not been investigated.

Ligand-dependent nuclear receptor peroxisome proliferator-activated receptor γ (PPARγ) can regulate transcription and expression of target genes. PPARγ can regulate phenotype of macrophages and participate in M2 macrophage polarization [12, 13]. Studies reported that PPARγ is expressed in macrophages and PPARγ ligands can induce expression of M2 macrophage markers in vitro [14]. One recent study found that SA attenuates cisplatin-induced nephrotoxicity by PPARγ activation [15]. This study intended to investigate the effect and underlying mechanism of SA on macrophage polarization and structural and neural remodeling after MI.

Materials And Methods

Animals and experimental group

All animal procedures were performed in agreement with the Animal Care and Use Committee of Renmin Hospital of Wuhan University (Wuhan, China) and complied with the guidelines of the National Institutes of Health for the care and use of laboratory animals. SD rats (male, 6-8 weeks) were randomly divided into the sham group (n = 10), MI group (n = 10), and MI+SA group (n = 10). In the MI+SA group, rats were treated with SA (Med Chem Express, USA) (20 mg/kg/d) by intragastric administration 24 h after acute MI for 1 week or 4 weeks. SA was dissolved in corn oil (5 mg/mL). The rats in the MI and sham groups were administered corn oil by intragastric administration.

Acute MI model establishment

Rats were anaesthetized with an intraperitoneal injection of sodium pentobarbital (50 mg/kg). The rats then underwent endotracheal intubation and surface electrocardiography. A thoracotomy was performed and the heart was exposed. Left anterior descending (LAD) coronary artery ligation was performed by a 6-0 noninvasive suture according to our previous method [16]. In the sham group, the suture was only crossed under the LAD coronary artery without ligation.

Cell culture and treatment

Bone marrow was isolated from femurs and tibias of rats according to our previous method [17]. Red blood cell lysate was added for 5 min and then washed with PBS. Cells were cultured in Dulbecco's modified Eagle's medium with 10% fetal bovine serum and 30 μg/L macrophage colony-stimulating factor. Following 48 h of culture in an incubator at 37°C with a 5% CO_2 atmosphere, the medium was removed and replaced with fresh medium every 3 days. BMDMs were randomly divided into six groups to observe the effect of SA on M2 polarization: a control group, IL-4 group, SA group, IL-4+SA group, SA+GW9662 group, and IL-4+SA+GW9662 group. BMDMs in the LPS group and IL-4 group were treated with LPS (100 ng/mL) or IL-4 (10 ng/mL) for 24 h. SA (100 or 200 μmol/L) were simultaneously added for 24 h. In SA+GW9662 and IL-4+SA+GW9662 group, BMDMs were pre-treated with PPARγ antagonist GW9662 (5 μmol/L)) (HY-16578, Med Chem Express, USA).

Echocardiography

Echocardiography was used to evaluate left ventricular (LV) systolic function after 1 week and 4 weeks. Echocardiography was recorded at the papillary muscle level in the LV short axis. The transducer frequency was 10 MHz. The parameters included LV end-diastolic dimension (LVEDD) and LV ejection fraction (LVEF).

Western blot analysis

Total protein was extracted from myocardial tissue in the peripheral zone of MI and BMDMs, and the BCA method was used to determine the protein concentration. Sodium dodecyl sulfate-polyacrylamide gel electrophoresis was performed, and the proteins were transferred to a polyvinylidene difluoride membrane. The membrane was incubated with primary antibodies against MCP-1 (Bioss, bs-34021R, 1:500), CCR2 (Biorbyt, orb378630, 1:1000), Arg-1 (Santa, sc-271430, 1:500), MMP-2 (Abcam, ab92536, 1:1000), MMP-9 (Abcam, ab76003, 1:1000), PPARγ (Abcam, ab209350, 1:1000) overnight at 4°C and then incubated with secondary antibody HRP-goat anti-rabbit (ASPEN, AS1107) at 37°C for 45 min; then, enhanced chemiluminescence detection was performed. Optical density was detected by the AlphaEaseFC software system.

Reverse transcription-quantitative polymerase chain reaction (RT-qPCR)

Total RNA was extracted from the peripheral area of infarction by using TRIzol® reagent. The isolated RNA was converted into cDNA using the PrimeScript™RT reagent kit with gDNA Eraser (TaKaRa, RR047A). The primers were synthesized by Invitrogen Biotechnology (Shanghai, China) and presented in Table 1. RT-qPCR was performed using the StepOne™ Real-Time PCR system (Life Technologies, Carlsbad, CA, USA). The reactions were then conducted using SYBR® Premix Ex Taq TM II (Takara Bio, Japan, RR420A). Semilog amplification curves were analyzed using the 2-ΔΔCt comparative quantification method, and the expression of each gene was normalized to GAPDH.

Table 1
PCR primers used in this study

Gene	Primer
TNF-α	Sense:5'- CACCACGCTCTTCTGTCTACTG - 3'
	Antisense:5'- GCTACGGGCTTGTCACTCG -3'
IL-1α	Sense:5'- GCAAAGAAATCAAGATGGCCA - 3'
	Antisense:5'- CATGAAGTGAGCCATAGCTTGC-3'
IL-1β	Sense:5'- GTGGCAGCTACCTATGTCTTGC - 3'
	Antisense:5'- CCACTTGTTGGCTTATGTTCTGT -3'
IL-10	Sense:5'- GCAGGACTTTAAGGGTTACTTGG - 3'
	Antisense:5'- ATCATTCTTCACCTGCTCCACT -3'
NGF	Sense:5'- AGAACCGTACACAGATAGCAATGTC - 3'
	Antisense:5'- GTCCTGTTGAAGGAGATTGTACCAT -3'
PPARγ	Sense:5'- CCCTTTACCACGGTTGATTTC - 3'
	Antisense:5'- CTTCAATCGGATGGTTCTTCG -3'
Arg-1	Sense:5'- AACACTCCCCTGACAACCA - 3'
	Antisense:5'- CATCACCTTGCCAATCCC -3'
GAPDH	Sense:5'- CGCTAACATCAAATGGGGTG -3'
	Antisense:5'- TTGCTGACAATCTTGAGGGAG -3'

Masson trichrome staining

The myocardial tissue in the peripheral infarct zones was fixed with 4% paraformaldehyde and embedded in paraffin. The sections were dewaxed, dehydrated, and stained with hematoxylin. Next, the sections were stained with Ponceau and aniline blue after washing and sealed with neutral gum. Collagen volume fraction (CVF) was defined as the ratio of collagen fiber area to the view area.

Immunofluorescence

The paraffin sections were dewaxed and hydrated, and then blocked with 5% bovine serum albumin (BSA) for 20 min. Next, the sections were incubated with the primary antibodies CD68 (Abcam, ab125212; 1:200) and CD206 (Abcam, ab64693; 1:200) overnight at 4°C and the secondary antibodies Cy3-conjugated AffiniPure goat anti-rabbit IgG (Aspen, AS11079) at 37°C for 50 min. 4',6-Diamidino-2-phenylindole (DAPI) was used to visualize the nuclei. The sections were observed by the ScanScope system. Four visual fields were randomly selected in every section. The CD68+ and CD206+ count was the number of CD68-positive cells and CD206-positive cells per field.

Immunohistochemistry

The primary antibodies TH (Abcam, ab109189, 1:200) and GAP43 (Abcam, ab128005, 1:150) were added to the sections overnight at 4°C. Then the sections were incubated with secondary antibody horseradish peroxidase-conjugated goat anti-rabbit IgG (Aspen, AS1107) at 37°C for 50 min. Then, the sections were stained with diaminobenzidine solution. Four visual fields were randomly selected in every section. The mean integral optical density of TH and GAP43 was measured by Image-Pro plus software.

Statistical analysis

The data are expressed as the mean ± SD. The statistical significance of the differences among groups was determined using one-way analysis of variance (ANOVA) with a Tukey post-hoc test. $P < 0.05$ was considered to indicate a statistically significant difference.

Results

SA ameliorated cardiac systolic dysfunction

In the MI group, LVEDD increased and LVEF decreased compared with the sham group after 1 week and 4 weeks (Fig. 1a-c). After SA treatment, LVEDD was reduced and LVEF were improved compared with the MI group. SA significantly ameliorated LV dysfunction after MI (Fig. 1a-c). There was no significant difference in LVEDD and LVEF between 1 and 4 weeks after myocardial infarction in the three groups.

SA reduced macrophages infiltration and promoted macrophage M2 polarization

The effect of SA on macrophage was analyzed at 1 week after MI. MCP-1/CCR2 plays an important role in migration and infiltration of macrophages after MI [18]. SA markedly reduced the increased MCP-1 and CCR2 protein levels after MI (Fig. 1d, e). The inflammatory factors TNF-α, IL-1α and IL-1β were declined in the MI+SA group compared with the MI group (Fig. 1f). The effect of SA on macrophage polarization was further analyzed and our study found that SA significantly enhanced M2 marker Arg-1 and IL-10 levels (Fig. 1d-f). Immunofluorescence analysis showed that the expressions of general macrophage marker CD68 and M2 macrophage marker CD206 were both upregulated in the MI group compared with the sham group. CD68 positive cells infiltration was greatly decreased and CD206 positive cells infiltration was greatly increased following SA treatment at 1 week after MI (Fig. 2a-c).

SA attenuated myocardial fibrosis

Myocardial fibrosis was evaluated by collagen synthesis and collagen degradation. Masson staining and quantitative analysis of CVF indicated that SA significantly attenuated interstitial fibrosis after 4 weeks of acute MI (Fig. 2d, e). MMP-2 and MMP-9 protein levels were also elevated after MI and markedly reduced after SA treatment (Fig. 2f, g).

Effect of SA on neural remodeling

Sympathetic nerve marker TH and nerve sprouting marker GAP43 were evaluated by immunohistochemistry. There was a small amount of TH-positive and GAP43-positive nerves in the sham group (Fig. 3a). At 4 weeks after MI, cardiac sympathetic nerve fibers and nerve sprouting were significantly increased in the peripheral area of MI (Fig. 3a-c). Compared with the MI group, the results of nerve density measurements indicated that TH-positive and GAP43-positive nerves were notably lower in the MI+SA group (Fig. 3a-c). Furthermore, SA inhibited NGF expression after MI. (Fig. 3d).

Effect of SA on the expression of PPARγ in vivo and effect of SA on BMDMs

The expression of PPARγ protein was upregulated at 1 week after MI. In the MI+SA group, PPARγ expression significantly elevated compared with the MI group (Fig. 4a, b). To further investigate the mechanism of SA on macrophage, we observed the effect of SA on BMDMs in vitro. Our study found that SA also acticvated expression of PPARγ mRNA in BMDMs and IL-4 induced BMDMs in a concentration-dependent manner (Fig. 4c). SA and IL-4 both enhanced Arg1 and IL-10 expressions, and there was no significant difference in Arg1 expression between the two groups. SA also elevated Arg1 and IL-10 levels in IL-4 induced BMDMs (Fig. 4d, e). The PPARγ antagonist GW9662 attenuated the SA and IL-4+SA induced M2 macrophage markers expressions (Fig. 4d, e).

Discussion

This study explored the influence of SA on macrophage polarization and ventricular remodeling in rat with MI model. We provide evidence for the following: (1) SA increased M2 macrophages infiltration after MI; (2) SA attenuated myocardial interstitial fibrosis and neural remodeling after MI; (3) In vitro study we further found that SA induced and promoted macrophage M2 polarization in BMDMs and IL-4 induced BMDMs; and (4) Activation of PPARγ is a potential mechanism by which SA regulates macrophage polarization.

The plasticity of macrophages makes macrophages an important regulatory target for the treatment of myocardial infarction. After myocardial infarction, pro-inflammatory M1 macrophages aggravate inflammatory response and myocardial injury by releasing pro-inflammatory cytokines, exosomes and miRNA [19]. An excessive inflammatory response and prolonged M1 macrophage accelerates myocardial injury and adverse cardiac remodeling [20, 21]. Previous studies have shown that SA can inhibit inflammation [5–7]. Our study found that SA can inhibit macrophage infiltration in peri-infarct area. MCP-1, a ligand of G protein coupled receptor CCR2, recruits monocytes to the infarcted myocardium and increases macrophage infiltration to promote the inflammatory microenvironment [22]. The expression of MCP-1 continuously markedly up-regulated from 1 day to 4 weeks after myocardial infarction, and MCP-1/CCR2 inhibition significantly ameliorates macrophage recruitment and interstitial fibrosis, and improves heart function after ischemia and reperfusion injury and MI [22, 23]. We found that SA not only downregulated the inflammatory factors TNF-α, IL-1α and IL-1β but also modulated macrophage polarization after MI. Our in vivo and in vitro experiments investigated that SA can promote the polarization of M2 macrophages. M2 macrophages infiltration begin to activate at 5 to 7 days after

myocardial infarction [24, 25], and we observe M2 macrophages at 1 week after MI and in IL-4 induced BMDMs. IL-4 was applied to modulate macrophage polarization toward an M2 phenotype. IL-4 administration can significantly increase M2 macrophages infiltration and reduce the area of myocardial infarction and improve cardiac function in mice with myocardial infarction, and this effect depends on M2 macrophages rather than the direct effect of IL-4 [26]. M2 macrophages can secrete various anti-inflammatory cytokines, such as IL-10 and IL-1RA. We speculate promoting M2 cell polarization is one of the important anti-inflammatory mechanisms of SA and SA did not affect the polarization of M1 macrophages.

A few weeks and months after MI, the imbalance of homeostasis and increase in extracellular matrix synthesis and deposition play an important role in structural remodeling. Previous studies have shown that SA prevents cardiac fibrosis in a hypertensive animal model [8]. Persistent inflammatory response recruits and activates myofibroblasts that synthesize extracellular matrix proteins, which are involved in myocardial remodeling. Our study demonstrated that not only cardiac fibrosis but also MMP-2 and MMP-9 expression was inhibited after SA treatment. MMP-2 and MMP-9 are key regulators of LV remodeling and were upregulated both in MI and heart failure [27]. In MMP2 and MMP9 knockout mice, LV enlargement and collagen accumulation were significantly attenuated after MI [28, 29]. Clinical studies have also shown that MMP-9 is an independent risk factor for heart failure after acute MI [30]. Our study indicated that MMP2 and MMP9 is a regulatory target of anti-fibrosis effect of SA. Interstitial fibrosis gradually leads to impaired cardiac function and eventually progresses to heart failure. Our study also demonstrated that ventricle dilatation and systolic dysfunction following MI were evidently ameliorated after SA treatment.

Inflammatory response contributes to sympathetic neural remodeling that plays an important role in cardiac arrhythmias and SCD after MI. Macrophages that synthesize and express NGF around sympathetic nerves participate in sympathetic sprouting after MI [31]. Inflammatory factor TNF-α and IL-1 β also directly regulate the expression of NGF [32]. Furthermore, macrophage reduction followed by intravenous injection of clodronate inhibited sympathetic hyperinnervation after MI [33]. NGF secretion decreased significantly after M2 polarization of microglia [34]. Another study showed that atorvastatin induced M2 macrophages and attenuated sympathetic hyperinnervation in rat post myocardial infarction [35]. SA may inhibit NGF expression and regulate sympathetic remodeling and nerve sprouting by alleviating inflammatory response.

PPARγ is closely associated with M2 polarization [12]. Some drugs, such as rosuvastatin and pioglitazone can improve M2 macrophage polarization by PPARγ activation [36, 37]. IL-4 stimulation can induce BMDMs to M2 polarized activation and elevate PPARγ expression [38]. In IL-4 stimulated PPARγ null BMDMs, the expression of M2 macrophage marker Arg-1 were reduced by nearly half [13]. More importantly, there is PPAR response element (PPRE) within upstream of Arg-1, Ym-1, and Fizz-1 promoter to regulate the transcription of target genes [12, 13]. One recent study found that SA possesses a PPARγ activation role and the antioxidant stress effect of sinapic acid was abolished by the PPARγ inhibitor BADGE [15]. In our study, we also found SA that activated PPARγ in BMDMs in a concentration-dependent

manner. More importantly, PPARγ antagonist GW9662 attenuated the IL-4 induced M2 macrophage markers expressions after SA treatment, which indicated that PPARγ is the core signaling pathway of SA in regulating macrophage polarization. However, the specific mechanism of SA-mediated PPARγ activation remains to be further studied.

In conclusion, SA alleviated inflammation by promoting M2 macrophage polarization via activating PPARγ pathway, and SA attenuated structural and neural remodeling by inhibiting inflammation. SA could be a therapeutic candidate for anti-inflammation and ventricular remodeling after MI.

Declarations

Data Availability

The data used to support the findings of this study are available from the corresponding authors upon request.

Funding This work was supported by the National Natural Science Foundation of China (Grant numbers 81970082 and 81970277).

Conflict of interest The authors declare that there are no conflict of interest associated with the manuscript.

Author Contributions All authors contributed to the study conception and design. MY, JX and QZ performed the experiments. MY and JX were responsible for drafting manuscript. KH and XW assisted in the design of the study and performed the statistical analysis. QYZ and KH revised the manuscript. KH and QYZ confirm the authenticity of all the raw data. All authors have read and approved the final version of the manuscript.

Ethical approval All animal procedures were performed in agreement with the Animal Care and Use Committee of Renmin Hospital of Wuhan University.

Consent to participate and publish All authors reviewed and approved the final version for publication.

References

1. Kim Y, Nurakhayev S (2021) Macrophage Polarization in Cardiac Tissue Repair Following Myocardial Infarction. Int J Mol Sci 22:2715. https://doi.org/10.3390/ijms22052715
2. Li CY, Li YG (2015) Cardiac Sympathetic Nerve Sprouting and Susceptibility to Ventricular Arrhythmias after Myocardial Infarction. Cardiology research and practice 2015:698368. https://doi.org/10.1155/2015/698368
3. Chen PS, Chen LS, Cao JM, Sharifi B, Karagueuzian HS, Fishbein MC (2001) Sympathetic nerve sprouting, electrical remodeling and the mechanisms of sudden cardiac death. Cardiovascular Res

50:409–416. https://doi.org/10.1016/s0008-6363(00)00308-4

4. Zhang Z, Tang J, Cui X, Qin B, Zhang J, Zhang L, Zhang H, Liu G, Wang W, Zhang J (2021) New Insights and Novel Therapeutic Potentials for Macrophages in Myocardial Infarction. Inflammation 44:1696–1712. https://doi.org/10.1007/s10753-021-01467-2
5. Ansari MA, Raish M, Ahmad A, Alkharfy KM, Ahmad SF, Attia SM, Alsaad AMS, Bakheet SA (2017) Sinapic acid ameliorate cadmium-induced nephrotoxicity: In vivo possible involvement of oxidative stress, apoptosis, and inflammation via NF-κB downregulation. Environ Toxicol Pharmacol 51:100–107. https://doi.org/10.1016/j.etap.2017.02.014
6. Shin DS, Kim KW, Chung HY, Yoon S, Moon JO (2013) Effect of sinapic acid against carbon tetrachloride-induced acute hepatic injury in rats. Arch Pharm Res 36:626–633. https://doi.org/10.1007/s12272-013-0050-5
7. Bin Jardan YA, Ansari MA (2020) Sinapic Acid Ameliorates Oxidative Stress, Inflammation, and Apoptosis in Acute Doxorubicin-Induced Cardiotoxicity via the NF-κB-Mediated Pathway. 2020:3921796. https://doi.org/10.1155/2020/3921796
8. Silambarasan T, Manivannan J, Krishna Priya M, Suganya N, Chatterjee S, Raja B (2014) Sinapic acid prevents hypertension and cardiovascular remodeling in pharmacological model of nitric oxide inhibited rats. PLoS ONE 9:e115682. https://doi.org/10.1371/journal.pone.0115682
9. Aldubayan MA, Ahmed AS (2020) Sinapic Acid Attenuates Cardiovascular Disorders in Rats by Modulating Reactive Oxygen Species and Angiotensin Receptor Expression. 2020:1436858. https://doi.org/10.1155/2020/1436858
10. Roy SJ, Mainzen Prince PS (2013) Protective effects of sinapic acid on cardiac hypertrophy, dyslipidaemia and altered electrocardiogram in isoproterenol-induced myocardial infarcted rats. Eur J Pharmacol 699:213–218. https://doi.org/10.1016/j.ejphar.2012.11.012
11. Silambarasan T, Manivannan J, Priya MK, Suganya N, Chatterjee S, Raja B (2015) Sinapic acid protects heart against ischemia/reperfusion injury and H9c2 cardiomyoblast cells against oxidative stress. Biochem Biophys Res Commun 456:853–859. https://doi.org/10.1016/j.bbrc.2014.12.022
12. Bouhlel MA, Derudas B, Rigamonti E, Dièvart R, Brozek J, Haulon S, Zawadzki C, Jude B, Torpier G, Marx N, Staels B, Chinetti-Gbaguidi G (2007) PPARgamma activation primes human monocytes into alternative M2 macrophages with anti-inflammatory properties. Cell Metabol 6:137–143. https://doi.org/10.1016/j.cmet.2007.06.010
13. Odegaard JI, Ricardo-Gonzalez RR, Goforth MH, Morel CR, Subramanian V, Mukundan L, Red Eagle A, Vats D, Brombacher F, Ferrante AW, Chawla A (2007) Macrophage-specific PPARgamma controls alternative activation and improves insulin resistance. Nature 447:1116–1120. https://doi.org/10.1038/nature05894
14. Penas F, Mirkin GA, Vera M, Cevey Á, González CD, Gómez MI, Sales ME, Goren NB (2015) Treatment in vitro with PPARα and PPARγ ligands drives M1-to-M2 polarization of macrophages from T. cruzi-infected mice. Biochim Biophys Acta 1852:893–904. https://doi.org/10.1016/j.bbadis.2014.12.019

15. Singh HP, Singh TG, Singh R (2020) Sinapic acid attenuates cisplatin-induced nephrotoxicity through peroxisome proliferator-activated receptor gamma agonism in rats. Journal of pharmacy & bioallied sciences 12:146–154. https://doi.org/10.4103/jpbs.JPBS_220_19
16. Yang M, Xiong J, Zou Q, Wang DD, Huang CX (2018) Chrysin attenuates interstitial fibrosis and improves cardiac function in a rat model of acute myocardial infarction. J Mol Histol 49:555–565. https://doi.org/10.1007/s10735-018-9793-0
17. Li Y, Yang M, Zhang G, Li L, Ye B, Huang C, Tang Y (2018) Transcription factor TBX18 promotes adult rat bone mesenchymal stem cell differentiation to biological pacemaker cells. Int J Mol Med 41:845–851. https://doi.org/10.3892/ijmm.2017.3259
18. Frangogiannis NG (2007) Chemokines in ischemia and reperfusion. Thromb Haemost 97:738–747
19. Liu S, Chen J, Shi J, Zhou W, Wang L, Fang W, Zhong Y, Chen X, Chen Y, Sabri A, Liu S (2020) M1-like macrophage-derived exosomes suppress angiogenesis and exacerbate cardiac dysfunction in a myocardial infarction microenvironment. Basic Res Cardiol 115:22. https://doi.org/10.1007/s00395-020-0781-7
20. Liu X, Chen J, Zhang B, Liu G, Zhao H, Hu Q (2019) KDM3A inhibition modulates macrophage polarization to aggravate post-MI injuries and accelerates adverse ventricular remodeling via an IRF4 signaling pathway. Cell Signal 64:109415. https://doi.org/10.1016/j.cellsig.2019.109415
21. Troidl C, Möllmann H, Nef H, Masseli F, Voss S, Szardien S, Willmer M, Rolf A, Rixe J, Troidl K, Kostin S, Hamm C, Elsässer A (2009) Classically and alternatively activated macrophages contribute to tissue remodelling after myocardial infarction. J Cell Mol Med 13:3485–3496. https://doi.org/10.1111/j.1582-4934.2009.00707.x
22. Hayashidani S, Tsutsui H, Shiomi T, Ikeuchi M, Matsusaka H, Suematsu N, Wen J, Egashira K, Takeshita A (2003) Anti-monocyte chemoattractant protein-1 gene therapy attenuates left ventricular remodeling and failure after experimental myocardial infarction. Circulation 108:2134–2140. https://doi.org/10.1161/01.cir.0000092890.29552.22
23. Liehn EA, Piccinini AM, Koenen RR, Soehnlein O, Adage T, Fatu R, Curaj A, Popescu A, Zernecke A, Kungl AJ, Weber C (2010) A new monocyte chemotactic protein-1/chemokine CC motif ligand-2 competitor limiting neointima formation and myocardial ischemia/reperfusion injury in mice. J Am Coll Cardiol 56:1847–1857. https://doi.org/10.1016/j.jacc.2010.04.066
24. Ben-Mordechai T, Palevski D, Glucksam-Galnoy Y, Elron-Gross I, Margalit R, Leor J (2015) Targeting macrophage subsets for infarct repair. J Cardiovasc Pharmacol Therap 20:36–51. https://doi.org/10.1177/1074248414534916
25. Mouton AJ, DeLeon-Pennell KY, Rivera Gonzalez OJ, Flynn ER, Freeman TC, Saucerman JJ, Garrett MR, Ma Y, Harmancey R, Lindsey ML (2018) Mapping macrophage polarization over the myocardial infarction time continuum. Basic Res Cardiol 113:26. https://doi.org/10.1007/s00395-018-0686-x
26. Shintani Y, Ito T, Fields L, Shiraishi M, Ichihara Y, Sato N, Podaru M, Kainuma S, Tanaka H, Suzuki K (2017) IL-4 as a Repurposed Biological Drug for Myocardial Infarction through Augmentation of

Reparative Cardiac Macrophages: Proof-of-Concept Data in Mice. Sci Rep 7:6877. https://doi.org/10.1038/s41598-017-07328-z

27. DeLeon-Pennell KY, Meschiari CA, Jung M, Lindsey ML (2017) Matrix Metalloproteinases in Myocardial Infarction and Heart Failure. Prog Mol Biol Transl Sci 147:75–100. https://doi.org/10.1016/bs.pmbts.2017.02.001
28. Ducharme A, Frantz S, Aikawa M, Rabkin E, Lindsey M, Rohde LE, Schoen FJ, Kelly RA, Werb Z, Libby P, Lee RT (2000) Targeted deletion of matrix metalloproteinase-9 attenuates left ventricular enlargement and collagen accumulation after experimental myocardial infarction. J Clin Investig 106:55–62. https://doi.org/10.1172/jci8768
29. Hayashidani S, Tsutsui H, Ikeuchi M, Shiomi T, Matsusaka H, Kubota T, Imanaka-Yoshida K, Itoh T, Takeshita A (2003) Targeted deletion of MMP-2 attenuates early LV rupture and late remodeling after experimental myocardial infarction. Am J Physiol Heart Circ Physiol 285:H1229–1235. https://doi.org/10.1152/ajpheart.00207.2003
30. Wagner DR, Delagardelle C, Ernens I, Rouy D, Vaillant M, Beissel J (2006) Matrix metalloproteinase-9 is a marker of heart failure after acute myocardial infarction. J Card Fail 12:66–72. https://doi.org/10.1016/j.cardfail.2005.08.002
31. Hasan W, Jama A, Donohue T, Wernli G, Onyszchuk G, Al-Hafez B, Bilgen M, Smith PG (2006) Sympathetic hyperinnervation and inflammatory cell NGF synthesis following myocardial infarction in rats. Brain Res 1124:142–154. https://doi.org/10.1016/j.brainres.2006.09.054
32. Takano S, Uchida K (2016) Nerve Growth Factor Regulation by TNF-α and IL-1β in Synovial Macrophages and Fibroblasts in Osteoarthritic Mice. 2016:5706359. https://doi.org/10.1155/2016/5706359
33. Wernli G, Hasan W, Bhattacherjee A, van Rooijen N, Smith PG (2009) Macrophage depletion suppresses sympathetic hyperinnervation following myocardial infarction. Basic Res Cardiol 104:681–693. https://doi.org/10.1007/s00395-009-0033-3
34. Zhou D, Ji L, Chen Y (2020) TSPO Modulates IL-4-Induced Microglia/Macrophage M2 Polarization via PPAR-γ Pathway. J Mol Neurosci 70:542–549. https://doi.org/10.1007/s12031-019-01454-1
35. Yang N, Cheng W, Hu H, Xue M, Li X, Wang Y, Xuan Y, Li X, Yin J, Shi Y, Yan S (2016) Atorvastatin attenuates sympathetic hyperinnervation together with the augmentation of M2 macrophages in rats postmyocardial infarction. Cardiovasc Ther 34:234–244. https://doi.org/10.1111/1755-5922.12193
36. Zhang T, Shao B, Liu GA (2017) Rosuvastatin promotes the differentiation of peripheral blood monocytes into M2 macrophages in patients with atherosclerosis by activating PPAR-γ. Eur Rev Med Pharmacol Sci 21:4464–4471
37. Zhang C, Zhang Y, Zhang C, Liu Y, Liu Y, Xu G (2019) Pioglitazone increases VEGFR3 expression and promotes activation of M2 macrophages via the peroxisome proliferator–activated receptor γ. Mol Med Rep 19:2740–2748. https://doi.org/10.3892/mmr.2019.9945
38. Ying W, Cheruku PS, Bazer FW, Safe SH, Zhou B (2013) Investigation of macrophage polarization using bone marrow derived macrophages. Journal of visualized experiments: JoVE 76:50323.

https://doi.org/10.3791/50323

Figures

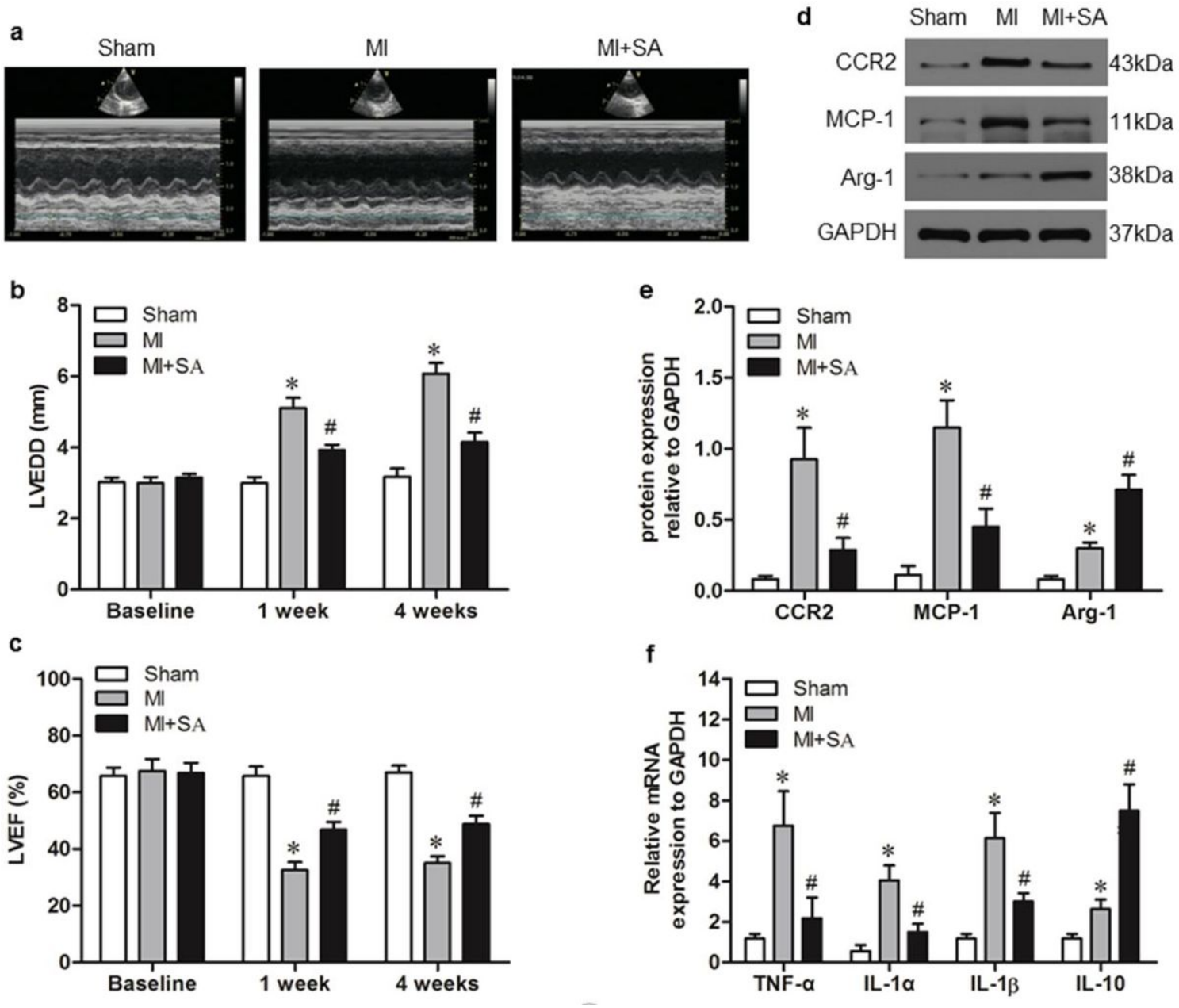

Figure 1

SA ameliorated cardiac dysfunction and modulated macrophage polarization and inflammatory factors after MI. **a** Echocardiographic images in the three groups at 1 week after MI. **b and c** SA decreased LVEDD and increased LVEF at 1 week and 4 weeks after MI. **d and e** MCP-1, CCR2 and M2 marker Arg-1 expressions in the three groups were detected by Western blot. **f** Levels of inflammatory factors TNF-α, IL-1α, IL-1β and IL-10 were detected by RT-PCR. *compared with the sham group, P <0.05, #compared with the MI+SA group, P <0.05

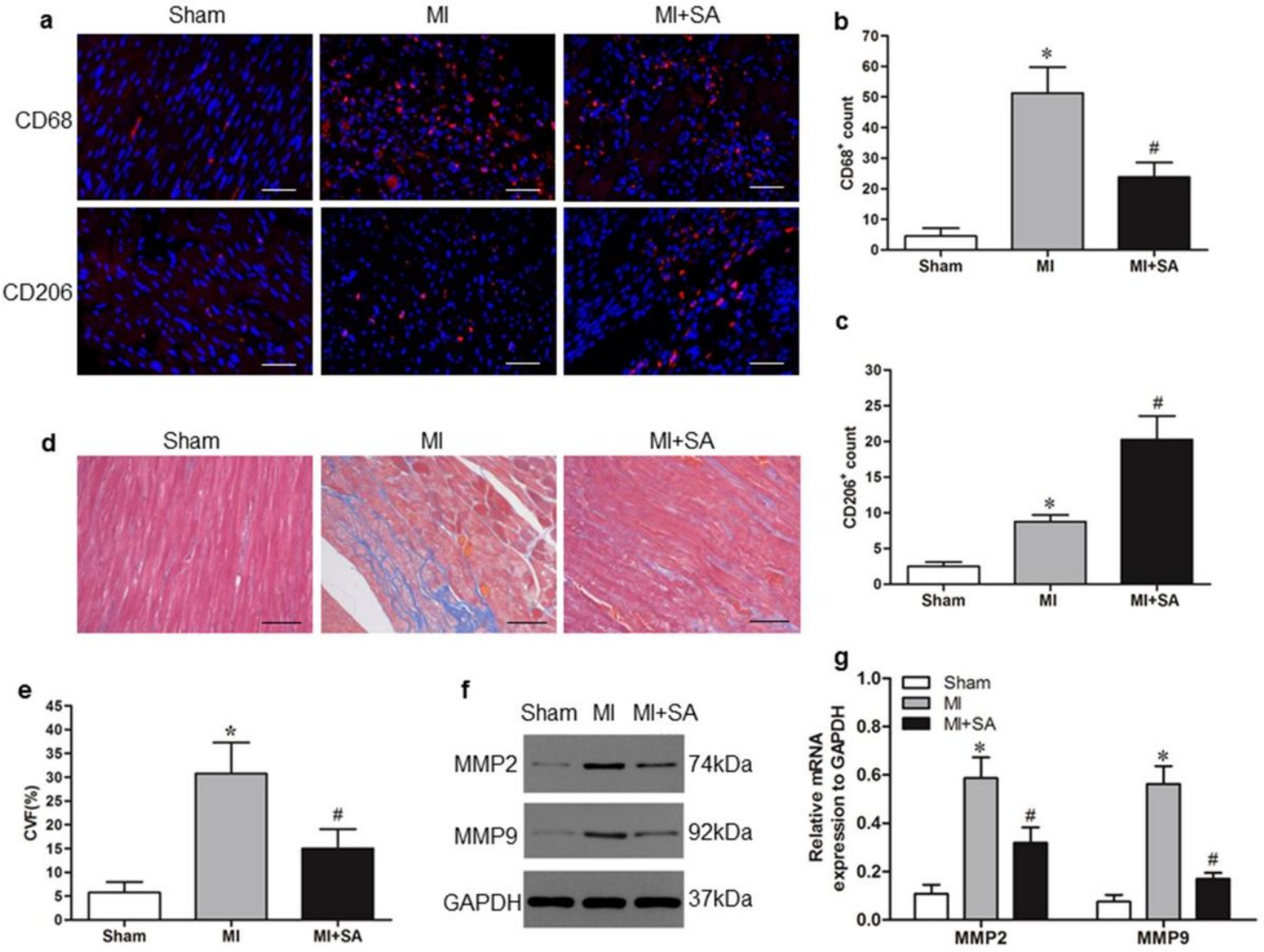

Figure 2

SA modulated macrophages infiltration at 1 week after MI and attenuated myocardial fibrosis at 4 week after MI. **a** The general macrophage marker CD68 and M2 macrophage marker CD206 were detected by immunostaining analysis. Positive staining of CD68 and CD206 is red. The nuclei were counterstained with DAPI (blue). Scale bar, 100 μm. **b and c** Immunostaining quantitative analysis showed that CD68 expression was decreased and CD206 expression was increased after SA treatment. **d** Interstitial fibrosis (blue) detected by masson staining in the sham group, MI group, and MI+SA group. Scale bar, 50 μm. **e** Comparison of collagen volume fraction (CVF). **f and g** Expression of MMP9 and MMP2 proteins in the three groups. *compared with the sham group, P <0.05, #compared with the MI+SA group, P <0.05

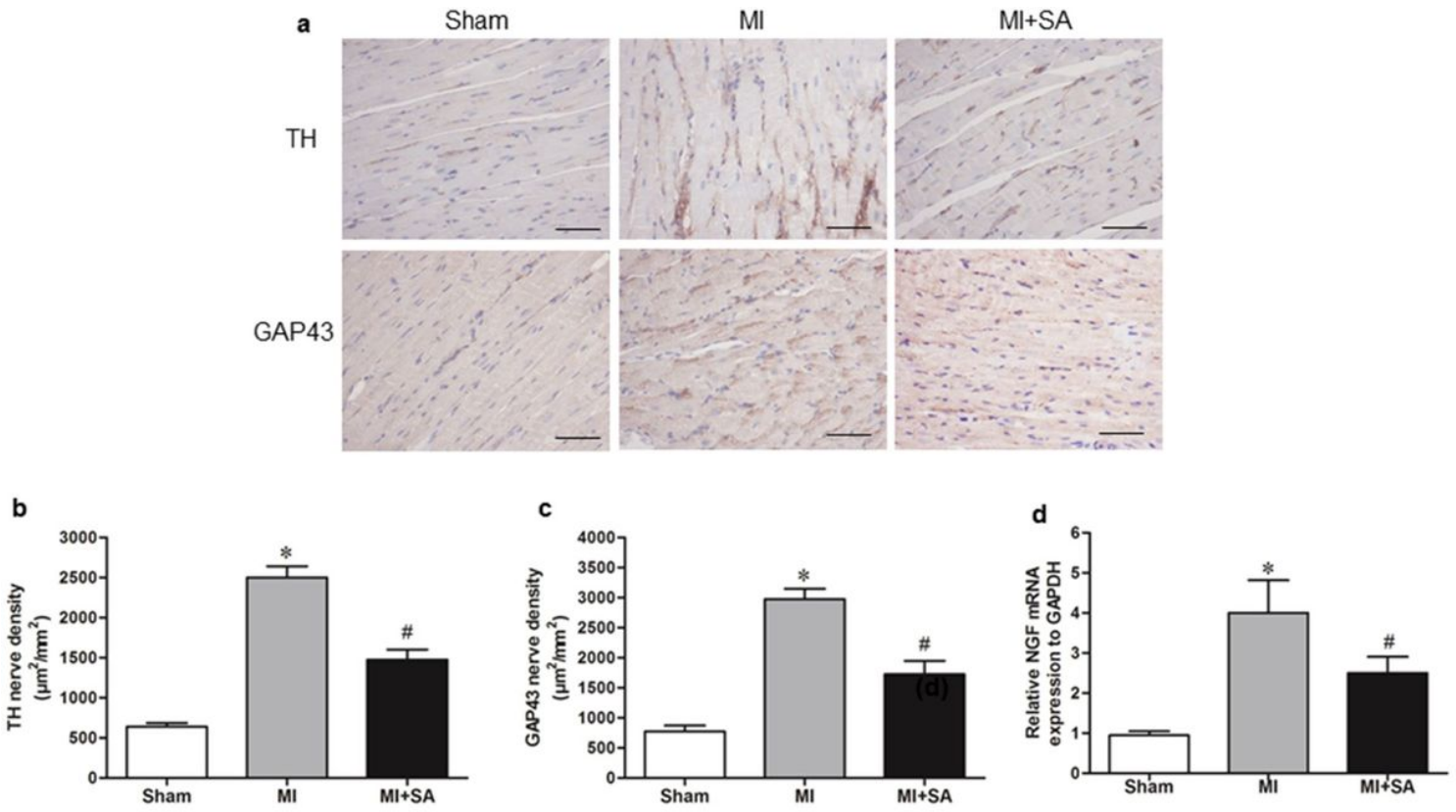

Figure 3

SA attenuated sympathetic nerve remodeling and nerve sprouting at 4 week after MI. **a** TH and GAP43 were detected by immunohistochemistry. Scale bar, 50 μm. **b and c** Quantitative analysis of TH and GAP43. **d** Expression of NGF mRNA in the three groups. *compared with the sham group, P <0.05, #compared with the MI+SA group, P <0.05

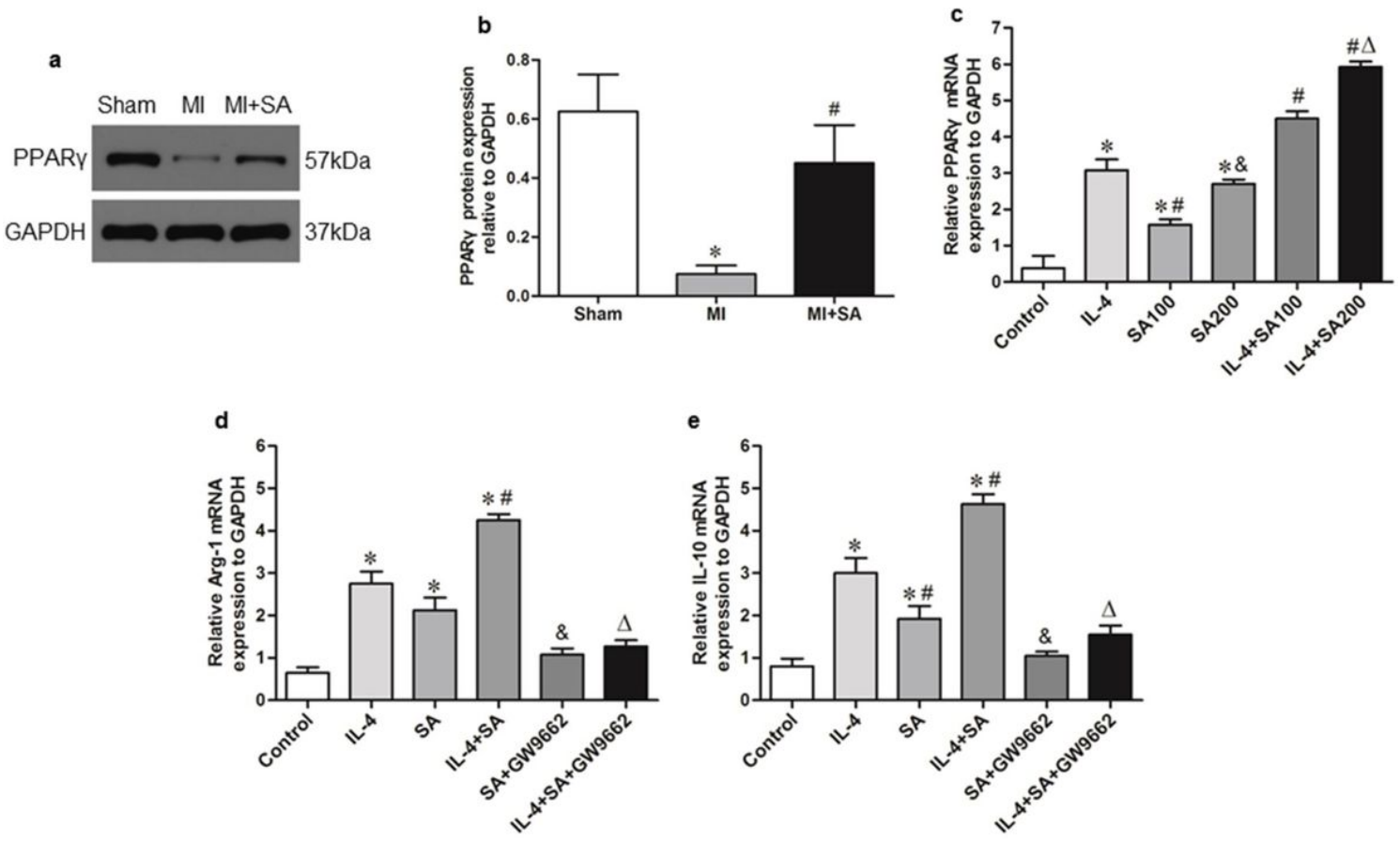

Figure 4

SA activated expression of PPARγ and the effect of SA on BMDMs. **a and b** PPARγ protein expression was detected by Western blot analysis. *compared with the sham group, P <0.05, #compared with the MI+SA group, P <0.05. **c** PPARγ mRNA expression in BMDMs and IL-4 induced BMDMs after SA treatment. *compared with the control group, P <0.05, #compared with the IL-4 group, P <0.05, &compared with the SA100 group, P <0.05; Δ compared with the IL-4+SA100 group, P < 0.05. **d and e** The effect of SA on Arg1 and IL-10 mRNA expressions in BMDMs and IL-4 induced BMDMs and the effect of PPARγ antagonist GW9662 on SA induced Arg1 and IL-10 expressions. *compared with the control group, P <0.05, #compared with the IL-4 group, P <0.05, &compared with the SA group, P <0.05; Δ compared with the IL-4+SA group, P <0.05